

Wear rate-state interaction modelling for a multi-component system: Models and an experimental platform

Roy Assaf*, Phuc Do**, Phil Scarf*, Samia Nefti-Meziani*

* University of Salford, Salford, M5 4WT, UK

e-mail: r.assaf@salford.ac.uk

** Université de Lorraine, Vandoeuvre-les-Nancy, 54506, France

e-mail: phuc.do@univ-lorraine.fr

Abstract: This paper proposes a general deterioration model for a multi-component system. The deterioration process of a component depends upon the operational conditions, the component's own state, and also the state of other components. An experimental platform that aims to provide more insight into the true nature of degradation of multi-component systems is also described. Some preliminary experimental results demonstrate the feasibility and advantages of the proposed deterioration model for describing highly stochastic degradation processes in industrial engineering.

© 2016, IFAC (International Federation of Automatic Control) Hosting by Elsevier Ltd. All rights reserved.

Keywords: Maintenance, degradation, rate-state interaction, multi-component system

1. INTRODUCTION

Predicting remaining useful lifetime is a key element for preventing failure of components, which incurs unexpected downtime leading to low plant efficiency and higher maintenance costs. However predicting remaining useful lifetime can be very challenging in a real world environment, due to the random nature of events that might happen and have an impact on the components degradation process. A key to having more accuracy while predicting these components' remaining useful lifetime is to be able to master their deterioration process. Many deterioration models have been proposed and successfully applied for various industrial systems, see Wang (2002) and Van Noortwijk (2009) for an overview. It is shown in the literature that the deterioration process may depend on the operational condition (load, temperature, vibration, humidity, maintenance operation, etc), see for instance Deloux et al. (2009), Song et al. (2014) and Do et al. (2015). It is also shown that the deterioration process of a system may depend on the current state of the system Si et al. (2012). However, in such works, the deterioration models can be only applied for single-component systems.

Industrial machines keep becoming more complex, containing multiple interacting components forming subsystems within a system as a whole. Taking into consideration dependencies between components when modelling the deterioration behaviours of multi-component systems has recently shown an increase in popularity among researchers. Degradation interaction or state dependence, which implies that the state evolution of a component depends on both its state and the state of other components, has been introduced in Bian and Gebraeel (2014) for prognostics of system lifetime, and in Do et al. (2015), Rasmekomen and Parlikad (2016) for maintenance optimization. However, these works do not consider the operational condition impacts on the deterioration modelling. To face this issue, the first objective of this paper is to

propose a general deterioration model for multi-component systems, which takes into account not only state dependence but also the operational condition effect. The second objective of the paper is to present an experimental platform developed, with the aim of providing the multi-component degradation model more insight about the true nature of deterioration for components with dependencies. In contrast with previous developed platforms, the experimental platform presented has sensors that are set up and configured in a way that would best capture wear interdependencies between components, the aim is to estimate the parameters of the presented degradation model in this paper.

Highly dynamic maintenance schedules are not well appreciated by OEMs and their clients, for logistic reasons among others. The experimental data that the developed platform will produce will compliment simulation data, and lead to more robust degradation models that in turn lead to more accurate remaining useful lifetime predictions, and thus more reliable maintenance scheduling can be done around that.

Some experimental platforms have been proposed and used to provide data for RUL calculations. A bearing accelerated degradation test bed has been developed at femto Nectoux et al. (2012), the test bed PRONOSTIA was aimed at validating methods related to bearing health assessment, this experimental platform provided 3 test sets for the PHM challenge on RUL predictions. A bearing test bed is proposed Yan et al. (2009) Vibration readings were collected using 3 accelerometers for the accelerated degradation test, and a new vibration signal analysis method was developed to extract wear related features. Similarly a Bearing test bed has been developed by the centre for intelligent maintenance systems, 4 bearings were installed on a single shaft, and 3 experiments ran to bearing failure, The Morlet wavelet filter-based de-noising method was applied for De-noising and extracting the weak signature from the noisy signal, and so perform reliable prognostics on the bearing data Qiu et al. (2006).

The remainder of this paper is organized as follows: The multi-component degradation model is presented in section 2, section 3 covers the developed experimental platform, some of the experimental data generated by the platform are presented in section 4 along with an analysis on the components' degradation dependence, and finally, section 5 concludes the paper.

2. MULTICOMPONENT SYSTEM MODELLING

Let us consider a system with multiple components interacting in series, where if one component fails the system fails. Each component i is subject to a continuous accumulation of deterioration in time, that is assumed to be described by a scalar random variable X_t^i . Component i fails if its deterioration level reaches the failure threshold L^i . When a component is not operating for whatever reason, its deterioration level remains unchanged during the stoppage period if no maintenance is carried out.

2.1 Rate-state interaction modelling

Between two adjacent maintenance activities, we assume that evolution of the deterioration level of component i is denoted by

$$X_{t+1}^i = X_t^i + \Delta X_t^i \quad (1)$$

Where ΔX_t^i is the increment in the degradation level of component i during one time unit.

From a practical point of view, the deterioration increment of a component at time t may depend on the operational condition (mission profile), its own current state as well as the current of state of other components. In this way, we suggest a general stationary model for the increment ΔX_t^i :

$$\Delta X_t^i = \Delta O_t^i + \Delta X_t^{ii} + \sum_{j \neq i} \Delta X_t^{ji} \quad (2)$$

where:

- ΔO_t^i is the increment in the deterioration level of component i caused by the operational condition during one time unit, namely the operation effect. ΔO_t^i may be specified as deterministic or as a random variable;
- ΔX_t^{ii} represents the increment in the deterioration level of component i induced by itself during one time unit, namely the intrinsic effect. This means that ΔX_t^{ii} depends only on the state of component i at time t . In the same manner, ΔX_t^{ii} may be specified as deterministic or as a random variable;
- ΔX_t^{ji} is the increment in the deterioration level of component i induced by component j during one time unit, called the interaction effect. ΔX_t^{ji} represents the state interaction between the two components j, i and may be specified as deterministic or as a random variable.

Several variants of the proposed model can be specified:

Case 1: $\Delta O_t^i > 0, \Delta X_t^{ii} = 0$ and $\Delta X_t^{ji} = 0$ with $\forall j \neq i$: neither intrinsic effect nor interaction effect and the proposed model becomes a basic model describing the homogenous

degradation behaviour of independent components, see for instance Van Noortwijk (2009).

Case 2: $\Delta O_t^i > 0, \Delta X_t^{ii} > 0$ and $\Delta X_t^{ji} = 0$ with $\forall j \neq i$: no interaction effect and the proposed model becomes a basic model describing the non-homogenous degradation behaviour, see Si et al. (2012).

Case 3: $\Delta O_t^i = 0, \Delta X_t^{ii} = 0$ and $\Delta X_t^{ji} > 0$ with $j \neq i$: here the components i and j ($j \neq i$) are stochastically dependent but the increment in the deterioration level of component i depends only on the state of component j . For this case, the proposed model corresponds to the model introduced in Rasmekomen and Parlikad (2016) where the interaction effect (ΔX_t^{ji}) is described by a normal distribution whose parameters depend on the deterioration level of component j .

Case 4: $\Delta O_t^i > 0, \Delta X_t^{ii} = 0$ and $\Delta X_t^{ji} > 0$ with $j \neq i$: components i and j ($j \neq i$) are stochastically dependent and the increment in the deterioration level of component i does not depends on the state of the component its self, see Do et al. (2015), Bian and Gebrael (2014).

Case 5: $\Delta O_t^i > 0, \Delta X_t^{ii} > 0$ and $\Delta X_t^{ji} > 0$ with $j \neq i$: the components i and j ($j \neq i$) are stochastically dependent and the increment in the deterioration level of component i depends on the operational condition, the state of component i as well as the state of component j .

As an example, we consider the case 4 and extend the model proposed for condition-based maintenance of a two-component system in Do et al. (2015) to multi-component systems. In that way,

$$\Delta X_t^i = \Delta O_t^i + \sum_{j \neq i} \mu^{ji} * (X_t^j)^{\sigma^{ji}} \quad (3)$$

where ΔO_t^i is described by a gamma law with shape parameter α^i and scale parameter β^i . μ^{ji} and σ^{ji} are non-negative real numbers that quantify the influence of component j on the deterioration rate of component i . Fig. 1 illustrates the degradation evolution of a 3-component system with rate-state interaction modelled by eq. (3) with

$$\alpha = \begin{pmatrix} \alpha^1 \\ \alpha^2 \\ \alpha^3 \end{pmatrix} = \begin{pmatrix} 4.944 \\ 4.350 \\ 5.193 \end{pmatrix}, \beta = \begin{pmatrix} \beta^1 \\ \beta^2 \\ \beta^3 \end{pmatrix} = \begin{pmatrix} 3.919 \\ 1.09 \\ 2.257 \end{pmatrix}$$

and,

$$\sigma = [\sigma^{ji}] = \begin{pmatrix} 0 & 0.54 & 0.729 \\ 0.785 & 0 & 0.836 \\ 0.838 & 0.555 & 0 \end{pmatrix},$$

$$\mu = [\mu^{ji}] = \begin{pmatrix} 0 & 0.254 & 0.108 \\ 0.384 & 0 & 0.346 \\ 0.242 & 0.118 & 0 \end{pmatrix}$$

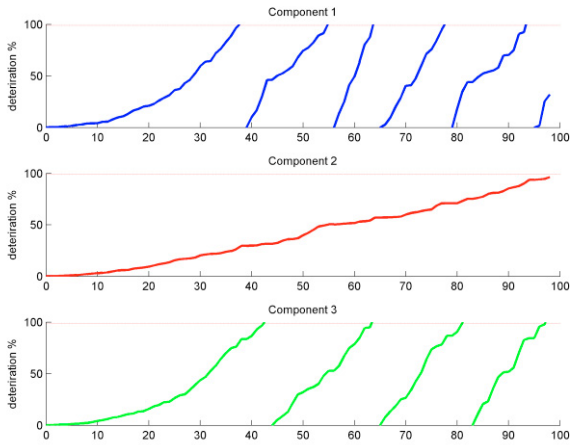


Fig. 1. Degradation evolution of a 3-component system with wear rate-state interaction.

3. DESCRIPTION OF EXPERIMENTAL PLATFORM

The experimentation platform (Fig. 2) aims to validate deterioration models for multiple component systems, giving more insight into the true nature of the degradation process for interacting parts with dependencies when set in a real world environment. The platform has been designed and developed at the Autonomous Systems and Robotics Lab at The University of Salford, using CAD (Computer Aided Design), 3D printing, the use of a lathe for cutting and preparing the reinforcement parts which are made out of metal for stiffening the platform and the use of an Arduino board based data acquisition system. The objective of this platform is to gather experimental data for multi-component degradation models, for the reason that multi-component systems with interdependencies follow a highly stochastic degradation process inherited by their complex mechanical design.

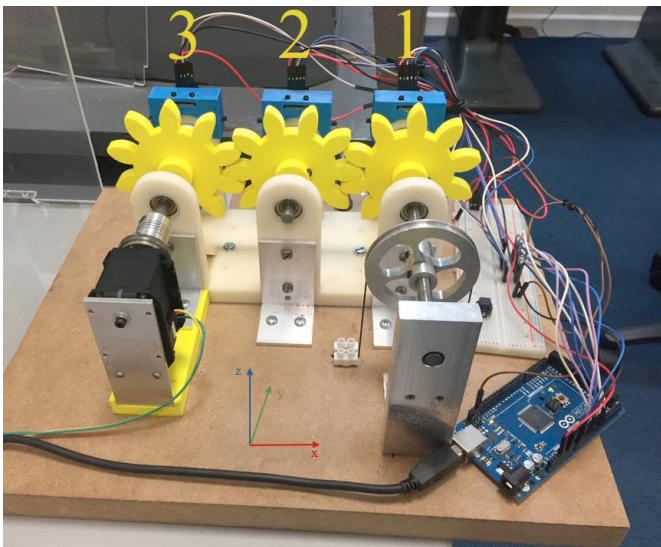


Fig. 2. The experimental platform.

This platform can test variable gear sizes made out of different material. The numbering of the mounted accelerometers as well as the orientation is as depicted in (Fig. 2). This experimental platform can be divided into 3 main parts, which are: the driving part, the load part and the data acquisition part. A detailed description is presented in the following subsections.

3.1 Driving part

This part consists of a fixed bracket which holds a continuous turn servo motor, and can be exchanged with different motor sizes and of different power. Feedback is collected on the driving servo motor including motor position which allows RPM (rounds per minute) to be measured, the load on the motor is also collected along with the motor's instantaneous temperature, which allows a failsafe threshold to be set and so prevent overheating. The motor is coupled with a shaft which drives the platform. That shaft is mounted with a gear that meshes with a second gear which in turn meshes with a 3rd gear forming a gear train. The 3 shafts are held each by two shaft support bearings on each side of the rig. We restrict translational movement of the shafts by using small washers that are in contact with the inner ring of the bearing from one side, and held in place by a 3D printed shaft collar on the other side, creating a frictionless rotation all while keeping the shaft in place, and thus prevent additional noise originating from uncalculated loads as a result of friction.

The installed motor has a stall torque of 7.3 N.m and can reach speeds up to 78 RPM. Both the speed and Torque can be set by the user using an SDK or a MATLAB script which in turn saves all commands and records motor operating speed, current usage, torque and load on motor.

3.2 Generation of the radial force

The load is being applied through a pulley system that resembles a dynamometer mechanism. The pulley is fixed on the last shaft, furthest from the driving shaft, which is in turn held in place by another shaft support bearing. A strong filament is wrapped around the pulley once, the filament is fixed at one side of the MDF (medium density foam), and attached on the other side to a load hook where some weights are hanged, and so provide the opposing torque on the motor thus creating a load that can be easily changed by changing the weights that are being held.

3.3 Measurements part

We are using 3 sensors to collect vibration data from this rig, these sensors are 3-axis accelerometers, and each mounted as close as possible to the centreline of the shaft support bearing, which avoids picking up distorted signals. This is realized by fixing the sensors in place using Hex Socket screws that pin the sensors to a 3D printed housing, which in turn is fixed on the rig using hex socket screws.

The 3 accelerometers each have a full sensing range of $\pm 3g$. These Accelerometers are connected to an Arduino Mega 2560 board, which converts the analogue signal into a 10bit digital signal with a value range of 0-1023, this board's sampling frequency can go up to a 10khz on 1 single channel.

The digital data is then transmitted to MATLAB via serial communication and a 2.0 USB port, using binary communication to make sure that the Baud Rate is never exceeded, and thus no information is lost. The sensor data is also coupled with Arduino’s internal microsecond clock, which provides us with the time at which the analogue signal was read, and so gives us a robust sampling time and sampling frequency, this can be used to switch from time domain to the frequency domain when processing the data.

4. PRELIMINARY RESULTS & ANALYSIS

4.1 Experimental setting

The data presented in this section is taken from the experimental platform after running it continuously for 2 hours. This data has a sample size of 1000 corresponding to 2.5159 Seconds of accelerometer readings. The load that is being applied to the system corresponds to 1N.m of opposing torque on the motor. The motor that was used to produce these results is the MX-67 from Dynamixel. The motor was running at 14.8V and had an average current intake of 0.66A and thus using 9.768Watts of Power. The running speed was 64-65 RPM. Using (4) and (5) we calculate that the motor produces a torque of 1.43 N.m.

$$P_{Watt} = V_{Volts} \times I_{Amps} \quad (4)$$

$$P_{Watt} = \tau_{N.m} \times \omega_{rad/s} \quad (5)$$

The gear train is made out of 3 gears meshing in series, all these gears have the same number of teeth, 10. The gears meshing frequency is calculated to be 10.83 Hz at a running speed of 65 RPM. The sampling frequency for this data is 397 Hz.

4.2 Experimental platform data

After receiving the raw data, we centre the readings to 0 and translate the digital signal from Arduino to a measurement in G’s and get (Fig. 3).

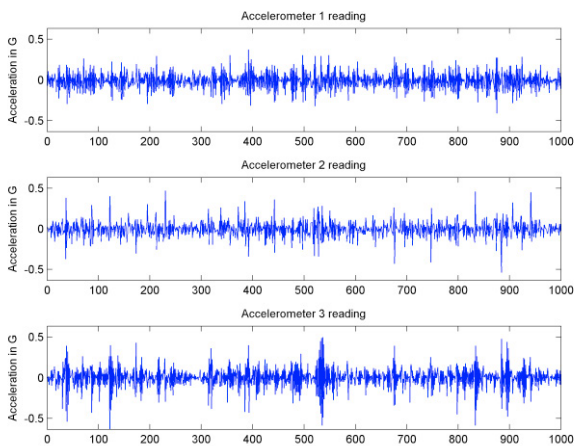


Fig. 3. Accelerometer signal from the x-axis of the accelerometers.

In (Fig. 4) we present the FFT (fast Fourier transform) of all 3 accelerometers in the x orientation, we also highlight the gear meshing frequency at 10.7 Hz and its harmonics, using the dashed red lines.

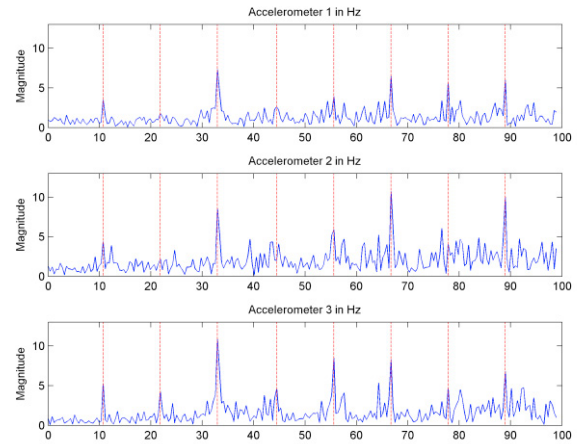


Fig. 4. FFT of accelerometers’ x-axis readings. Gear Meshing frequency and harmonics are highlighted in red.

4.3 Multi-Component interaction

It is important to point out that each accelerometer is mounted over the shaft supporting its respective gear, and so accelerometer 1’s signal corresponds mainly to gear 1 and so on. Also, it is important to note that an increase in vibration intensity measured for a certain gear will lead to a decrease in efficiency when it comes to power transmission, that is caused by the absorption of some of the power being transferred and so the vibrating gear would then be experiencing more forces leading to faster degradation.

To measure dependencies between system components the following experiment was carried out:

- Only x-axis accelerometer data was collected, freeing 6 channels from analogue to digital conversion and thus raising the sampling frequency to 655Hz per accelerometer.
- Tooth surface wear was induced into gear number 3 uniformly on all 10 teeth.
- The induced tooth wear on gear number 3 happened in 4 stages, where at each successive stage the wear was slightly increased.

The experimentation platform ran at each stage after inducing wear, and the accelerometers data was collected. The raw data was then cleaned and transformed into readings in G’s. Then the signal’s envelope was computed to give a clear indication of the change in vibration intensity (Fig. 5). We used the Hilbert transform to get the envelope of our vibration signal, the Hilbert transform takes the FFT of the vibration signal, zeroes out the negative frequencies, and does performs an IFFT (inverse FFT). The absolute value of the real and imaginary parts of the transform is the envelope.

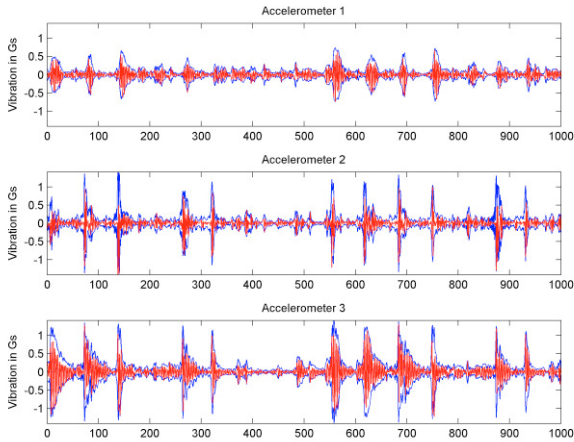


Fig. 5. Accelerometer data after wear stage 4, acceleration signal in red and envelope in blue.

In (Fig. 5), the envelope of the vibration signal shows a greater amplitude in accelerometer 3 when compared to the other 2 accelerometers, and if we sum up the values of the envelopes, we would then have a higher value for accelerometer 3 which is a clear indicator of the now elevated vibration intensity due to wear. Some statistical properties for the accelerometer signals were also computed along with the sum of the signal envelopes, and are presented as wear state indicators of the gears in (Fig. 6).

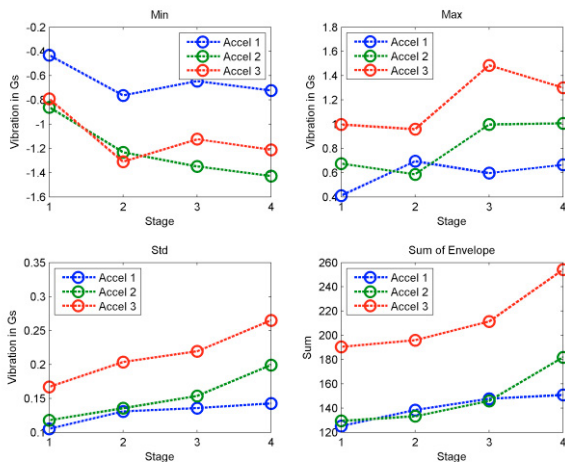


Fig. 6. Component wear state indicators of all 3 gears at the 4 wear stages

We can see that after inducing wear on the teeth of gear 3, we get on average a higher maximum value and lower minimum value for gear 3 indicating an increase in the range of vibration, and thus higher vibration intensity. This increase in vibration intensity is represented even clearer when we look at the standard deviation and the sum of the envelope of the signal, we can see that there is always an increase in these 2 indicators the more we induce wear onto gear 3.

The dependency between the 3 components is shown similarly in (Fig. 6), after analysing the standard deviation

present in the lower left corner, and the sum over the envelope values at each stage. We see that an increase in wear in gear 3 has a strong positive correlation with the increase in vibration in gear 2, with which it is in direct contact and so has direct dependence, and a smaller positive correlation with gear 1's vibration level, where there is an indirect contact and so an indirect dependence is present. This dependence can be clearly illustrated if we take the difference between vibration intensity, indicated by the standard deviation or the sum over the signal's envelope, from one stage to another, and so we can check how much variation in vibration is incurred after each stage of inducing wear on gear number 3.

5. CONCLUSIONS

This paper presents a mathematical model for multi-component degradation modelling, which takes into account rate-state interaction between components. The main idea of the proposed model is that the deterioration increment of a component may depend on the operational condition (mission profile), its own current state, as well as the current of state of other components. Thanks to its flexibility, the proposed model covers different existing deterioration models. An experimental platform which aims to provide more insight into the true nature of degradation of multi-component systems is also presented. Some preliminary experimental results are also presented and discussed. The experimental results shows that rate-state interaction between the components exists: a clear correlation of increased vibration intensity is shown in section 4.

Future work includes continuous runs to failure of the experimental platform in different contexts, to get continuous data which will be fitted with the proposed model. Furthermore, we will also focus on the development of a hybrid prognostic model based on the mathematical model presented in this paper and a data driven approach, which would lead to more accurate RUL estimations, and in turn lead to developing robust optimal maintenance strategies.

ACKNOWLEDGMENT

The research leading to these results has received funding from the People Programme (Marie Curie Actions) of the European Union's Seventh Framework Programme FP7/2007-2013/ under REA grant agreement number 608022.

REFERENCES

- Bian, L. and Gebraeel, N. (2014) Stochastic framework for partially degradation systems with continuous component degradation-rate-interactions. *Naval Research Logistics*, 61(4), pp.286-303.
- Deloux, E. and Castanier, B. and Bérenguer C. (2009) Predictive maintenance policy for a gradually

- deteriorating system subject to stress. *Reliability Engineering & System Safety*, 94 (2):418-431.
- Do, P., Scarf, P. and Iung, B. (2015) Condition-based maintenance for a two-component system with dependencies. *IFAC-PapersOnLine*, 48(21), pp.946-951.
- Do P., Voisin A., LEVRAT E. and IUNG, B. (2015) A proactive condition-based maintenance strategy with both perfect and imperfect maintenance actions. *Reliability Engineering & System Safety*, 133: 22-32
- Nectoux, P., Gouriveau, R., Medjaher, K., Ramasso, E., Chebel-Morello, B., Zerhouni, N. and Varnier, C. (2012) PRONOSTIA: An experimental platform for bearings accelerated degradation tests. *In IEEE International Conference on Prognostics and Health Management, PHM'12.* (pp. 1-8).
- Qiu, H., Lee, J., Lin, J. and Yu, G. (2006) Wavelet filter-based weak signature detection method and its application on rolling element bearing prognostics. *Journal of sound and vibration*, 289(4), pp.1066-1090.
- Rasmekomen, N and Parlikad, AK (2016) Condition-based maintenance of multi-component systems with degradation state-rate interactions. *Reliability Engineering & System Safety*, 148. pp. 1-10.
- Song, S. and Coit, D.W. and Feng, O. (2014) Reliability for systems of degrading components with distinct component shock sets. *Reliability Engineering & System Safety*, 132:115-124.
- Van Noortwijk. J. (2009) A survey of the application of Gamma processes in maintenance. *Reliability Engineering and System Safety*, 94:2–21.
- X. Si, W. Wang, , C. Hu, D.-H. Zhou, and M.-G. Pecht. (2012) Remaining useful life estimation based on a nonlinear diffusion degradation process. *IEEE Transactions on reliability*, 6:50–67.
- Wang, H. (2002) A survey of maintenance policies of deteriorating systems. *European journal of operational research*, 139(3):469–489.
- Yan, R. and Gao, R.X. (2009) Multi-scale enveloping spectrogram for vibration analysis in bearing defect diagnosis. *Tribology International*, 42(2), pp.293-302.